DALTON

Syntheses of several kinds of one-dimensional nickel(II)-nitrito complexes: a new μ-nitrito nickel(II) alternating chain

Albert Escuer,*,†,[a] Ramon Vicente[a] and Xavier Solans[b]

[a] *Departament de Química Inorgànica, Universitat de Barcelona. Diagonal, 647. 08028-Barcelona, Spain*

[b] *Departament de Cristal.lografia i Mineralogia, Universitat de Barcelona, Martí Franqués s/n, 08028-Barcelona, Spain*

Three new one-dimensional μ-nitrito nickel(II) complexes of formula $[\{NiL^1(\mu\text{-}NO_2)\}_n][ClO_4]_n$ **1**, $[\{NiL^2(\mu\text{-}NO_2)\}_n][ClO_4]_n$ **2** and $[\{NiL^3(\mu\text{-}NO_2)\}_n][ClO_4]_n$ **3** have been synthesized and characterized [L^1 = *N*,*N*′-bis(2-aminoethyl)propane-1,3-diamine, L^2 = *N*,*N*′-bis(3-aminopropyl)ethane-1,2-diamine, L^3 = *N*,*N*′-bis(3-aminopropyl)propane-1,3-diamine]. Complex **3** crystallizes in the triclinic system, space group $P\bar{1}$, with $a = 10.747(3)$, $b = 9.413(2)$, $c = 8.789(2)$ Å, $\alpha = 95.52(2)$, $\beta = 108.98(3)$, $\gamma = 106.83(3)°$, $Z = 2$, $R = 0.058$. The nickel atom is placed in an octahedral environment with the μ-nitrito groups in *trans* position co-ordinated by the nitrogen atom and to the neighbouring nickel by one of its oxygen atoms. Inversion centres on the nitrito bridges but not on the nickel atoms allow an alternating system, whereas compounds **1** and **2** appear to be homogeneous one-dimensional chains. The three compounds show antiferromagnetic behaviour, with very similar *J* values of -27.4 cm^{-1} for **1**, -32.3 cm^{-1} for **2** and -31.8 cm^{-1} for **3**. Magnetic properties have been rationalized by means of extended-Hückel molecular orbital calculations.

In the last few years the research in our laboratory has been focused on the study of the interaction between paramagnetic centres in coupled systems in which the metal ions [mainly copper or nickel(II)] are relatively far from each other through bridging ligands like oxalato,[1] oxamidate,[2] carbonate[3] or end-to-end pseudo-halide ligands (azide,[4] cyanate,[5] thio-[6] or selenocyanate[7]). In these compounds the paramagnetic centres are typically separated by 5–6 Å, and the magnetic behaviour is strongly dependent on the bridging group, generally showing antiferromagnetic interactions, which can be considered strong or even very strong in some cases. The coupling in this kind of system may be modulated in two ways: by effecting changes in the environment of the metal ion by modification of the geometry of the co-ordination polyhedra,[2] or by modifying the bonding parameters related to the bridging ligand.[4] In both cases, magnetostructural correlations by means of extended-Hückel calculations give satisfactory explanations of the antiferromagnetic behaviour. In the present study our attention is centred on the nickel polynuclear systems with bridging nitrite as ligand. Several related di-,[8] tri-,[9] penta-,[10] hepta-nuclear[11] and one-dimensional systems[12–14] have been described. Considerable attention has been devoted to one-dimensional systems, for which only three very similar compounds $[\{Ni(en)_2(\mu\text{-}NO_2)\}_n]X_n$ (X = ClO_4^- or I_3^-; en = ethane-1,2-diamine), $[\{Ni(pn)_2(\mu\text{-}NO_2)\}_n][ClO_4]_n$, (pn = propane-1,3-diamine) and $[NMe_4][Ni(NO_2)_3]$, have been studied from structural and magnetic perspectives. These compounds show very similar magnetic behaviours, being antiferromagnetically coupled with *J ca.* -30 cm^{-1} independently of the structural differences. In the past few years these three compounds have been extensively investigated in order to study the Haldane gap effect.[15]

In this work, we increase the number of related one-dimensional nickel(II)–nitrito systems which show a single nitrito bridge by means of the syntheses of the new compounds $[\{NiL^1(\mu\text{-}NO_2)\}_n][ClO_4]_n$ **1**, $[\{NiL^2(\mu\text{-}NO_2)\}_n][ClO_4]_n$ **2** and $[\{NiL^3(\mu\text{-}NO_2)\}_n][ClO_4]_n$ **3** in which L^1, L^2 and L^3 are the tetramines *N*,*N*′-bis(2-aminoethyl)propane-1,3-diamine, *N*,*N*′-bis(3-aminopropyl)ethane-1,2-diamine and *N*,*N*′-bis(3-aminopropyl)propane-1,3-diamine respectively. Compounds **1** and **2** are homogeneous chains, whereas **3** is one of the few examples of magnetic and structural alternating systems with local spin $S = 1$.[16] Extended-Hückel molecular orbital (MO) calculations have been made in an attempt to explain the finding that the pseudo-constant *J* value in the one-dimensional nickel–nitrito systems is practically independent of the experimental variations in the bond parameters.

Experimental

CAUTION: Perchlorate salts of metal complexes with organic ligands are potentially explosive. Only a small amount of material should be prepared, and handled with caution.

Syntheses

To a concentrated aqueous solution of 2 mmol of L^1, L^2 or L^3 (*ca.* 30 cm^3) and $Ni(ClO_4)_2{\cdot}6H_2O$ (2 mmol) was added $NaNO_2$ (2 mmol) dissolved in water (10 cm^3). Slow evaporation of the resulting solutions gave reddish brown crystals of the corresponding one-dimensional compounds, suitable for X-ray determination in the case of **3** (*ca.* 70% yield) (Found: C, 21.8; H, 5.3; Cl, 9.6; N, 18.1. Calc. for $C_7H_{22}ClN_5NiO_6$ **1**: C, 22.0; H, 5.8; Cl, 9.25; N, 18.3. Found: C, 25.3; H, 5.8; Cl, 9.2; N, 18.5. Calc. for $C_8H_{22}ClN_5NiO_6$ **2**: C, 25.4; H, 5.85; Cl, 9.35; N, 18.5. Found: C, 27.3; H, 6.1; Cl, 9.0; N, 17.7. Calc. for $C_9H_{24}ClN_5NiO_6$ **3**: C, 27.55; H, 6.15; Cl, 9.05; N, 17.85%).

Spectral and magnetic measurements

Infrared spectra were recorded on a Nicolet 520 FTIR spectrophotometer. Magnetic measurements were carried out on a polycrystalline sample with a pendulum-type magnetometer (Manics DSM8) equipped with a helium continuous-flow cryostat working in the 4.2–300 K range, and a Drusch EAF 16UE electromagnet. The magnetic field was approximately 15000 G (1.5 T). Susceptibility data for compound **3** were measured on an MPMS Quantum Design instrument with a SQUID detector. Diamagnetic corrections were estimated from Pascal tables.

† WWW: ub.es/inorgani/molmag.htm

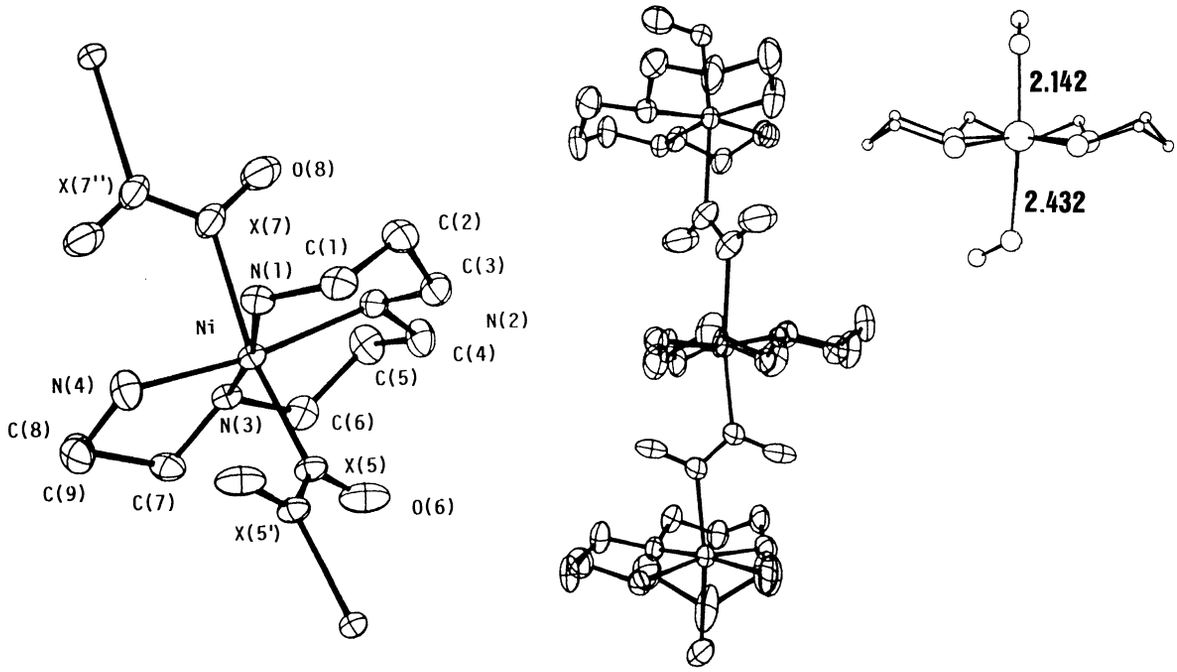

Fig. 1 Atom labelling scheme and a view of the chain for $[\{NiL^3(\mu\text{-}NO_2)\}_n][ClO_4]_n$ **3**. On the right, a view of a monomeric fragment showing the two different Ni–X bond distances is displayed

Crystallography

A prismatic crystal (0.1 × 0.1 × 0.2 mm) of compound **3** was selected and mounted on a Philips PW-1100 diffractometer. Unit-cell parameters were determined from automatic centring of 25 reflections and refined by the least-squares method. Intensities were collected at 298 K with graphite-monochromatized Mo-Kα radiation (λ 0.710 69 Å), using the ω–2θ scan technique. Three reflections were measured every 2 h as orientation and intensity control; significant intensity decay was not observed. Lorentz-polarization but not absorption corrections were made. The crystallographic data, conditions used for the intensity data collection, and some features of the structure refinement are listed in Table 1. The structure was solved by Patterson synthesis, using the SHELXS 86 computer program,[17] and refined by full-matrix least squares with SHELXL 93.[18] The function minimized was $\Sigma w\left||F_o|^2 - |F_c|^2\right|^2$, where $w = [\sigma^2(I) + (0.0735P)^2 + 2.7689P]^{-1}$, and $P = (|F_o|^2 + 2|F_c|^2)/3$. Values of f, f' and f'' were taken from ref. 19. The NO_2 groups were disordered giving Ni–ON(O)–Ni and Ni–N(O)O–Ni bridges in the same crystallographic site. A symmetry centre was found in the middle of the N–O bond. An occupancy factor of 0.5 was assigned to disorder positions according to the heights of the peaks in the Fourier synthesis and to the symmetry centre. The extinction coefficient was 0.076(16). All H atoms were computed and refined with an overall isotropic thermal parameter using a riding model. The final R (on F) factor was 0.058, wR (on $|F^2|$) = 0.148, goodness of fit 0.989 for all observed reflections. 3327 Reflections were measured in the range 3.63–30.00°. 3245 Reflections were assumed as observed applying the condition $[I > 2\sigma(I)]$. Number of parameters 212. Maximum and minimum shift/e.s.d. 0.0, mean peaks in the final difference synthesis were 1.085 and −1.195 e Å^{-3} respectively.

Attempts to solve the crystal structure of $[\{NiL^2(\mu\text{-}NO_2)\}_n][ClO_4]_n$ **2** were unsuccessful due to the poor quality of the crystals and the disorder found for the nitrito bridges, the C atoms of the L^2 ligand and the perchlorate counter anion. The space group found was $P2_1$, cell parameters $a = 8.759(3)$, $b = 17.330(4)$, $c = 5.306(2)$ Å, $\beta = 107.78(3)°$. From the structural and magnetic point of view, the 2_1 axis along the chain permits us to assume compound **2** is a magnetically homogeneous system.

Atomic coordinates, thermal parameters, and bond lengths and angles have been deposited at the Cambridge Crystallographic Data Centre (CCDC). See Instructions for Authors, *J. Chem. Soc., Dalton Trans.*, 1997, Issue 1. Any request to the CCDC for this material should quote the full literature citation and the reference number 186/306.

Results and Discussion

Structures of $[\{NiL^3(\mu\text{-}NO_2)\}_n][ClO_4]_n$ 3

In a general fashion, the structure consists of one-dimensional *trans*-nickel nitrito chains with the tetraamine ligands in equatorial position, isolated by ClO_4^- counter anions. No hydrogen bonds are present between the chains or perchlorate groups. The nitrito groups are disordered as is common in this kind of compound. The nitrite ligand is found in a disordered position in X(5)–X(5′) and X(7)–X(7″) sites (X = N or O). An occupancy factor of 0.5 was assigned to these disorder positions according to the peak heights in the Fourier synthesis and symmetry centres. The atom labelling of a monomeric unit and a view of the chain are shown in Fig. 1 and the main bond distances and angles are in Table 2. The most interesting feature of this compound is the inversion centres placed between the X(5)–X(5′) and X(7)–X(7″) atoms of the nitrito groups but not on the nickel atoms, giving a structurally alternating chain. Each Ni^{II} is co-ordinated by one L^3 and two nitrite ligands in a distorted-octahedral *trans* arrangement. The four N atoms of L^3 are in the same plane [maximum deviation 0.025 Å for N(2) and N(5)], whereas the nickel(II) ion is also 0.159 Å above the mean plane towards the X(5) position. Five of the bond lengths of the nickel environment [Ni–N(1) 2.104(4), Ni–N(2) 2.145(4), Ni–N(3) 2.132(4), Ni–N(4) 2.106(5) and Ni–X(5) 2.142(3) Å] are similar, and shorter than the remaining Ni–X(7) distance of 2.432(6) Å (Fig. 1). The nickel environment bond angles related to the nitrite ligands are Ni–X(5)–X(5′) 124.5(4) and Ni–X(7)–X(7′) 127.5(8)°. Each fragment of four Ni–X(7)–X(7)–Ni′ or Ni–X(5)–X(5)–Ni′ atoms is strictly planar, but in this case the dihedral angle between neighbouring Ni–X–X–Ni planes is 46.2°.

It is difficult to explain why the Ni–X(7) bond length is so long, but this experimental finding compares well with that for

Table 1 Crystallographic data for $[\{NiL^3(\mu\text{-}NO_2)\}_n][ClO_4]_n$ **3**

Formula	$(C_9H_{24}ClN_5NiO_6)_n$
M	394.51
Crystal symmetry	Triclinic
Space group	$P\bar{1}$
a/Å	10.747(3)
b/Å	9.413(2)
c/Å	8.789(2)
α/°	95.52(2)
β/°	108.98(3)
γ/°	106.83(3)
U/Å^3	786.8(3)
Z	2
D_c/g cm^{-3}	1.665
μ(Mo-Kα)/cm^{-1}	14.39
R [a]	0.058
wR [b]	0.148

[a] $R(F_o) = \Sigma||F_o| - |F_c||/\Sigma|F_o|$. [b] $wR(F_o)^2 = [\Sigma w(|F_o|^2 - |F_c|^2)^2/\Sigma w|F_o|^4]^{\frac{1}{2}}$.

Table 2 Selected bond distances (Å) and angles (°) for compound **3**; X = N or O, occupancy factor = 0.5

Nickel environment			
N(1)–Ni	2.104(4)	N(4)–Ni	2.106(5)
N(2)–Ni	2.145(4)	X(5)–Ni	2.142(3)
N(3)–Ni	2.132(4)	X(7)–Ni	2.432(6)
N(2)–Ni–N(1)	90.3(2)	N(4)–Ni–N(3)	90.5(2)
N(3)–Ni–N(1)	169.3(2)	X(5)–Ni–N(3)	92.7(1)
N(4)–Ni–N(1)	84.5(2)	X(7)–Ni–N(3)	84.4(2)
X(5)–Ni–N(1)	97.3(2)	X(5)–Ni–N(4)	95.9(2)
X(7)–Ni–N(1)	86.4(2)	X(7)–Ni–N(4)	93.8(2)
N(3)–Ni–N(2)	93.4(1)	X(7)–Ni–X(5)	170.0(2)
N(4)–Ni–N(2)	171.4(2)	Ni–X(5)–X(5′)	124.5(4)
X(5)–Ni–N(2)	91.5(2)	Ni–X(7)–X(7′)	127.5(8)
X(7)–Ni–N(2)	79.1(2)		
Nitrito bridge			
O(8)–X(7′)	1.175(11)	X(7′)–X(7″)	1.190(10)
X(5)–X(5′)	1.277(6)	O(8)–X(7′)	1.175(11)
O(6)–X(5)	1.203(8)		
O(6)–X(5)–X(5′)	116.7(5)	O(8)–X(7)–X(7″)	113.9 (10)

the $[\{NiL^3(\mu\text{-}N_3)\}_n][ClO_4]_n$ compound,[16b] in which a similar set of *trans*-'short–long' bond lengths for the two Ni–N (azido) distances of 2.077(3) and 2.204(3) Å was found. The *trans* co-ordination of the L^3 ligand, seems to generate preferentially systems in which the co-ordination polyhedron around the nickel atom is axially distorted to pseudo-square pyramidal geometry which may be related to the formation of three six-membered rings C_3N_2Ni in the same plane. Currently, we are trying to obtain new *trans*-NiL^3 derivatives in order to study this fact.

Magnetic results

The magnetic susceptibilities *vs.* T of $[\{NiL^1(\mu\text{-}NO_2)\}_n][ClO_4]_n$ and $[\{NiL^2(\mu\text{-}NO_2)\}_n][ClO_4]_n$ are plotted in Fig. 2 and χ_m and $\chi_m T$ *vs.* T for $[\{NiL^3(\mu\text{-}NO_2)\}_n][ClO_4]_n$ in Fig. 3. The χ_m value (3.98×10^{-3}, 4.07×10^{-3} and 4.30×10^{-3} cm^3 mol for **1**–**3** respectively, at room temperature) increases when the temperature decreases, reaching a broad maximum at *ca.* 50–55 K for the three complexes, with values of 9.26×10^{-3} for **1**, 7.62×10^{-3} for **2** and 8.81×10^{-3} cm^3 mol for **3**. These maximum values and positions indicate a similar moderate antiferromagnetic coupling between nickel(II) ions through the NO_2^- bridge. For **1** and **2**, the χ_m *vs.* T curve decreases continuously, and tends to zero at low temperatures.

Owing to the disorder observed along the chain, three different NiN_6, NiN_5O and NiN_4O_2 environments for the nickel ions are possible, but no effect as a consequence of an alternance of similar Lande factors along the chain is detectable at low temperatures as predicted by Drillon and co-workers.[20] On the other hand, in spite of this disorder, the bridging Ni–NO_2–Ni fragments are always equivalent and only one J superexchange parameter is expected. Consequently, the chains should be considered as strictly uniform for compounds **1** and **2**.

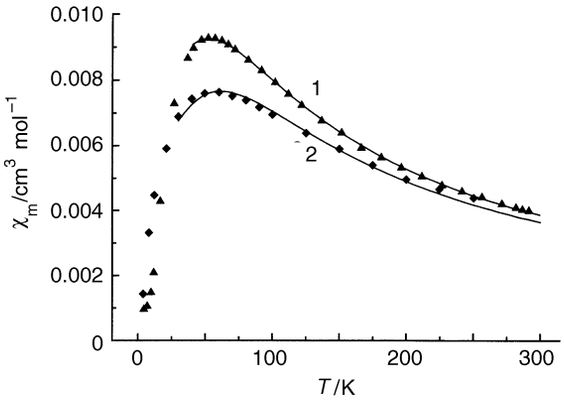

Fig. 2 Plots of χ_m *vs.* T of polycrystalline samples of $[\{NiL^1(\mu\text{-}NO_2)\}_n][ClO_4]_n$ **1** and $[\{NiL^2(\mu\text{-}NO_2)\}_n][ClO_4]_n$ **2**. Solid lines show the best fits obtained with the Weng equation

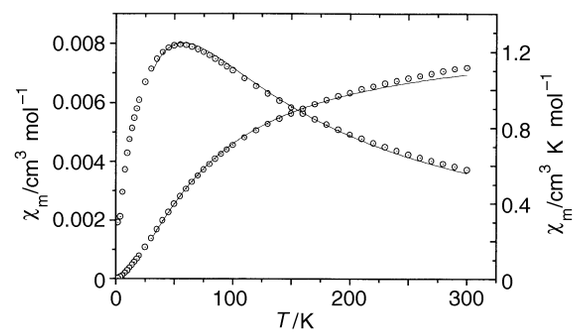

Fig. 3 Plots of χ_m and $\chi_m T$ *vs.* T for a polycrystalline sample of $[\{NiL^3(\mu\text{-}NO_2)\}_n][ClO_4]_n$ **3**. The solid lines show the best fit under the conditions described in the text

For compounds **1** and **2** the experimental data have been fitted by the Weng equation (1),[21] based upon the spin Hamiltonian

$$\chi_m = (N\beta^2 g^2/kT)(2 + A\gamma + B\gamma^2)/(3 + C\gamma + D\gamma^2 + E\gamma^3) \quad (1)$$

$H = -J\Sigma S_i S_{i+1}$, where the nickel ion is assumed to be magnetically isotropic, in which $A = 0.019$, $B = 0.777$, $C = 4.346$, $D = 3.232$, $E = 5.834$ and $\gamma = |J|/kT$. The fit is only possible up to near the maximum (in our case up to *ca.* 40 K), because neither zero-field splitting nor the Haldane gap is taken into account in the equation. The J value was obtained by minimizing the function $R = \Sigma(\chi_m^{calc} - \chi_m^{obs})^2/\Sigma(\chi_m^{obs})^2$. The best fitting parameters obtained were $J = -27.4$ cm^{-1}, $g = 2.36$, $R = 2.7 \times 10^{-5}$ for complex **1** and $J = -32.3$ cm^{-1}, $g = 2.33$, $R = 2.7 \times 10^{-4}$ for **2**. The good fits obtained with the above expression also confirm the homogeneous character of chains **1** and **2**. As was found for $[\{Ni(en)_2(\mu\text{-}NO_2)\}_n][ClO_4]_n$ and $[\{Ni(pn)_2(\mu\text{-}NO_2)\}_n][ClO_4]_n$, the low-temperature behaviour of the susceptibility plot differs from that expected for a gapless one-dimensional antiferromagnet, for which χ_0/χ_{max} should be slightly smaller than 1 for any local S. The experimental χ_0/χ_{max} were only 0.10 for **1** and 0.28 for **2** at 4–5 K, indicating the existence of the Haldane effect. From susceptibility measurements performed on powdered samples the E_G value cannot be quantified, but can only be assumed to be lower than $0.4|J|$.

Attempts to use equation (1) to adjust the experimental susceptibility data gave a poor fit for compound **3**, as expected

Table 3 Structural parameters (distances in Å, angles in °) for the one-dimensional nickel(II) compounds with a single nitrito bridge characterized to date. General formula $[\{Ni(N_4)(\mu\text{-}NO_2)\}_n]X_n$. The (NO) parameters refer to the disordered nitrito bridges

	$[\{Ni(en)_2(\mu\text{-}NO_2)\}_n]X_n$		$[\{Ni(pn)_2(\mu\text{-}NO_2)\}_n]X_n$	**3**
	X = ClO_4^-	X = I_3^-	X = ClO_4^-	X = ClO_4^-
Ni–N	2.163(4)	—	2.159(3)	—
Ni–O	2.183(4)	—	2.282(3]	—
Ni–(NO)	—	2.200(9)	—	2.142(3) 2.432(6)
N–O	1.249(5)	1.20(2)	1.257(4)	1.277(6) 1.190(10)
O–N–O	111.5(3)	109.7(12)	116.3(3)	116.7(5) 113.9(10)
Ni–N–O	121.1(3)	—	127.7(3)	—
Ni–O–N	127.9(3)	—	130.9(3)	—
Ni–(NO)–(NO)	—	129.3(3)	—	124.5(4) 127.5(8)
J/cm^{-1}	−33.0	−31.9	−36.0	−31.8, $\alpha = 0.88$
Ref.	12	12	13, 23	This work

from the structural data. For an alternating system with local $S = 1$, the analytical expression (2)[22] derived from the Hamilto-

$$\chi_m = (2/3)(N\mu^2 g^2/kT)(Ax + Bx^2 + Cx^3)/(1 + Dx + Ex^2 + Fx^3) \quad (2)$$

nian $H = -J_1(\Sigma S_{2i}S_{2i+1} + \alpha\Sigma S_{2i}S_{2i-1})$ may be applied, in which $x = |J_1|/kT$ and the terms A–F are functions of $\alpha = J_2/J_1$, with different values for the 0–0.5 and 0.5–1 ranges of α. This equation is strictly applicable for antiferromagnetic alternate chains with good approximation up to $kT/|J| = 0.4$. By using it the values of the coupling parameters were optimized up to $J = -31.8$ cm^{-1}, $g = 2.30$, alternance factor $\alpha = 0.88$, $R = 1.9 \times 10^{-4}$ for **3**.

Magnetostructural correlations

In Table 3 we present the main structural and magnetic features for the four one-dimensional nickel–nitrito systems with a single nitrito bridge reported to date. The bond angles and distances in the bridging region show significant differences but the J parameter is homogeneous for all compounds. In order to establish a wider magnetostructural correlation between J and the bond angle Ni–N–O and Ni–X bond distances, extended-Hückel MO calculations were performed by means of the CACAO program,[24] on a dimeric fragment modelled as shown in Scheme 1.

From the chosen axis, both symmetric and antisymmetric MOs with x^2–y^2 contribution are placed perpendicularly to the chain axis and do not interact with the MOs of the nitrito group, are degenerate and do not contribute to the exchange pathway. In contrast, the symmetric MO with z^2 contribution interacts with the last occupied MO of the nitrite ligand, whereas the antisymmetric combination of the corresponding z^2 atomic orbitals mainly interacts with a low-energy MO of the bridge.

The MO correlation diagram for the Ni–N–O angles between 110 and 140° for both MOs with z^2 contribution (Fig. 4) shows that the energy levels $\varphi z^2_{(s)}$ and $\varphi z^2_{(a)}$ are only slightly dependent on the bond angle. This result is not surprising, taking into account the symmetry of these MOs (Fig. 4), for which the antibonding interaction must be constant for experimental bond angles due to the pseudo-spherical shape of the active MOs of the nitrito group. The most important feature of this correlation diagram is that the gap between the levels $\varphi z^2_{(s)}$ and $\varphi z^2_{(a)}$ is constant and independent of the bond angle. According to Hoffmann and co-workers,[25] the antiferromagnetic component of J is proportional to the square of the gap (Δ^2) within

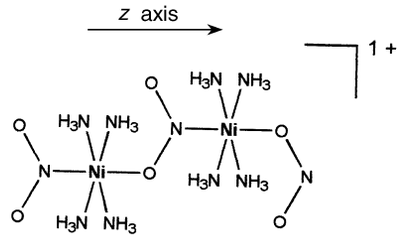

Scheme 1 Ni–NH_3 2.1, N–O 1.25, Ni–N, Ni–O between 2.1 and 2.4 Å; Ni–N–O, Ni–O–N between 110 and 140° (see text)

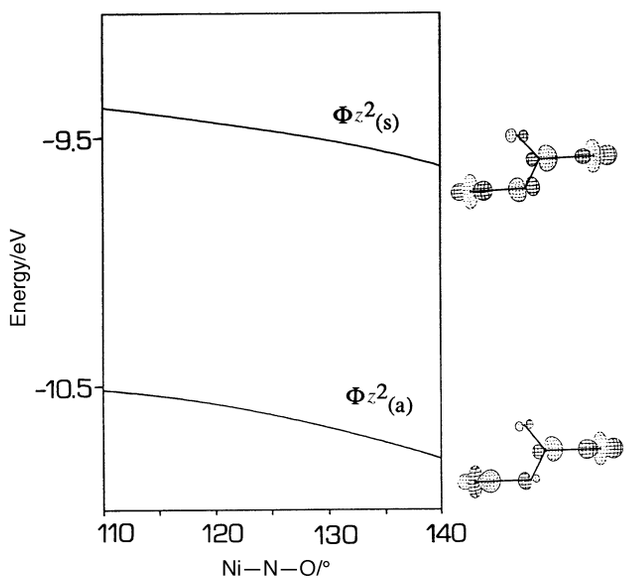

Fig. 4 The MO correlation diagram for the significant magnetic orbitals for a $[(NH_3)_5Ni\text{–}NO_2\text{–}Ni(NH_3)_5]^{3+}$ system as a function of the Ni–N–O bond angle. eV ≈ 1.60×10^{-19} J

$\varphi z^2_{(s)}$–$\varphi z^2_{(a)}$ [taking into account that the gap between the MO pair $\varphi x^2\text{-}y^2_{(s)}$–$\varphi x^2\text{-}y^2_{(a)}$ takes a zero value]; Δ^2 is practically constant and consequently the J value must also be constant irrespective of the bond parameters for a Ni–NO_2–Ni system bridged through the N and one of the O atoms, as is found experimentally.

The effect of the bond distance on the J_{AF} contribution also is poorly relevant; the antibonding character of the two $\varphi z^2_{(s)}$–$\varphi z^2_{(a)}$ MOs decreases when the bond length increases, due to the loss of overlap between the atomic orbitals of the bridge and the nickel atoms, but the two levels decrease in a similar fashion for the reasons indicated above for the bond-angle variation, and the Δ^2 value decreases only slightly. This is consistent with the experimental value of the alternance parameter $\alpha = 0.88$ found for compound **3**. According to these results the slightly lower coupling of −28.0 cm^{-1} should be assigned to the long bond-distance pathway whereas the J value of −31.8 cm^{-1} should correspond to the short bond-distance pathway.

The above results can be summarized in a general conclusion: the magnetic behaviour for this kind of nitrito chain is only slightly sensitive to the structural differences in the bond parameters of the bridging fragment, in good agreement with the experimental data. Bridging ligands for which there is a typical J value are generally rigid (such as the oxalato bridge, for example), and always show similar bond parameters, but the present co-ordination mode of the nitrito bridge has the unusual feature of practically constant superexchange properties for a non-rigid ligand.

Acknowledgements

This work was financially supported by the Comisión Interministerial de Ciencia y Technologia (PB93/0772).

References

1 A. Escuer, R. Vicente, M. S. El Fallah and J. Jaud, *Inorg. Chim. Acta*, 1995, **232**, 151 and refs. therein.
2 A. Escuer, R. Vicente, J. Ribas, R. Costa and X. Solans, *Inorg. Chem.*, 1992, **31**, 2627 and refs. therein.
3 A. Escuer, R. Vicente, S. B. Kumar, X. Solans, M. Font-Bardia and A. Caneschi, *Inorg. Chem.*, 1996, **35**, 3094.
4 R. Vicente, A. Escuer, J. Ribas, M. S. El Fallah, X. Solans and M. Font-Bardia, *Inorg. Chem.*, 1995, **34**, 1278 and refs. therein.
5 A. Escuer, R. Vicente, M. S. El Fallah, X. Solans and M. Font-Bardia, *J. Chem. Soc., Dalton Trans.*, 1996, 1013.
6 R. Vicente, A. Escuer, J. Ribas and X. Solans, *J. Chem. Soc., Dalton Trans.*, 1994, 259.
7 R. Vicente, A. Escuer, J. Ribas, X. Solans and M. Font-Bardia, *Inorg. Chem.*, 1993, **32**, 6117.
8 A. J. Finney, M. A. Hitchman, C. L. Raston, G. L. Rowbotton and A. H. White, *Aust. J. Chem.*, 1981, **34**, 2125; A. Gleizes, A. Meyer, M. A. Hitchman and O. Kahn, *Inorg. Chem.*, 1982, **21**, 2257.
9 D. M. L. Goodgame, M. A. Hitchman and D. F. Marsham, *J. Chem. Soc. A*, 1971, 259.
10 A. J. Finney, M. A. Hitchman, C. L. Raston, G. L. Rowbotton and A. H. White, *Aust. J. Chem.*, 1981, **34**, 2139; J. Ribas, C. Diaz, M. Monfort and J. Vilana, *Inorg. Chim. Acta*, 1984, **90**, L23; J. Ribas, C. Diaz, M. Monfort, J. Vilana, X. Solans and M. Font-Altaba, *Transition Met. Chem.*, 1985, **10**, 340.
11 M. S. El Fallah, E. Rentschler, A. Caneschi, R. Sessoli and D. Gatteschi, *Inorg. Chem.*, 1996, **35**, 3723.
12 A. Meyer, A. Gleizes, J. J. Girerd, M. Verdaguer and O. Kahn, *Inorg. Chem.*, 1982, **21**, 1729.
13 J. P. Renard, M. Verdaguer, J. Ribas, W. G. Stirling and C. Vettier, *J. Appl. Phys.*, 1988, **63**, 3538.
14 L. K. Chou, K. A. Abboud, D. R. Talham, W. W. Kim and M. W. Meisel, *Chem. Mater.*, 1994, **6**, 2051.
15 M. Sieling, W. Palme and B. Luthi, *Z. Phys. B Condensed Matter*, 1995, **96**, 297.
16 (*a*) R. Vicente, A. Escuer, J. Ribas and X. Solans, *Inorg. Chem.*, 1992, **31**, 1726; (*b*) A. Escuer, R. Vicente, J. Ribas, M. S. El Fallah, X. Solans and M. Font-Bardia, *Inorg. Chem.*, 1994, **33**, 1842; (*c*) A. Escuer, R. Vicente, X. Solans and M. Font-Bardia, *Inorg. Chem.*, 1994, **33**, 6007; (*d*) R. Vicente and A. Escuer, *Polyhedron*, 1995, **14**, 2133; (*e*) J. Ribas, M. Monfort, B. K. Ghosh, X. Solans and M. Font-Bardia, *J. Chem. Soc., Chem. Commun.*, 1995, 2375.
17 G. M. Sheldrick, *Acta Crystallogr., Sect. A*, 1990, **46**, 467.
18 G. M. Sheldrick, SHELXL 93, University of Göttingen, 1993.
19 *International Tables for X-Ray Crystallography*, Kynoch Press, Birmingham, 1974, vol. 4, pp. 99–110, 149.
20 E. Coronado, M. Drillon, A. Fuertes, D. Beltrán, A. Mosset and J. Galy, *J. Am. Chem. Soc.*, 1986, **108**, 900.
21 C. Y. Weng, Ph.D. Thesis, Carnegie Institute of Technology, 1968.
22 J. J. Borrás-Almenar, E. Coronado, J. Curely and R. Georges, *Inorg. Chem.*, 1995, **34**, 2704.
23 Dr J. Ribas, University of Barcelona, personal communication.
24 CACAO, Computed Aided Composition of Atomic Orbitals, version 4.0, C. Mealli and D. M. Proserpio, *J. Chem. Educ.*, 1990, **67**, 3399.
25 J. P. Hay, J. C. Thibeault and R. Hoffmann, *J. Am. Chem. Soc.*, 1975, **97**, 4884.

Received 1*st May* 1996; *Paper* 6/03070J